

Ground and Singlet Excited State Pyridinic Protonation of N₉-Methylbetacarboline in Water-N, N-Dimethylformamide Mixtures

Antonio Sánchez Coronilla · Carmen Carmona ·
María A. Muñoz · Manuel Balón

Received: 9 January 2009 / Accepted: 5 June 2009 / Published online: 18 June 2009
© Springer Science + Business Media, LLC 2009

Abstract The ground and the singlet excited state pyridinic protonation of 9-methyl-9H-pyrido[3,4-b]indole, MBC, in water-N,N-dimethylformamide mixtures has been studied by absorption, steady state and time resolved fluorescence measurements. These proton transfer reactions elapse by a stepwise mechanism modulated by different hydrogen bonded adducts and exciplexes formed by water molecules and the pyridinic nitrogen atom of the MBC. Based in the present and previous studies, a general mechanistic Scheme for the ground and the singlet excited state MBC pyridinic protonation has been proposed. Accordingly, in the ground state, upon increasing the water proportion of the water-N, N-dimethylformamide mixtures, a hydrogen bonded complex, HBC, its hydrogen bonded proton transfer complex, PTC, a pre-cationic complex, PC, and the cation, C, are progressively formed. In the excited state, MBC, HBC and PC behave as independent fluorophores. Excited state cations, C*, are mainly formed by direct excitation of the ground state cations and, in minor proportion, by the excited state reaction of the PTC* through the CL* exciplex.

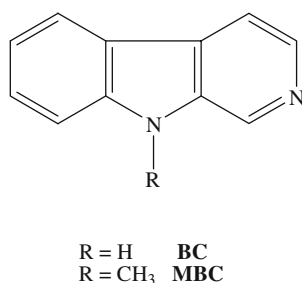
Keywords Betacarboline · Proton-transfer · Excited state · Water-N,N-dimethylformamide

Introduction

Betacarbolines, 9H-pyrido[3,4-b]indoles, are a family of fluorescent drug-binding alkaloids widely distributed in nature. Betacarboline derivatives occur in plants, tobacco and marijuana smokes, well-cooked foodstuffs and they are presumably formed in animals, including humans, as mammalian alkaloids [1-3]. Due to the wide range of biological properties displayed by these alkaloids, the interactions of carbolines with biological receptors are subjects of considerable interest. Carbolines are potent reversible inhibitors of the monoamine-oxidase enzyme (MAO) and they interact with a great number of neurotransmitters and neuromodulators of the Central Nervous System (CNS) [4-6]. They can also act as intercalating DNA drugs and possess cytotoxic properties [7-10], which are enhanced upon excitation with long-wave ultraviolet radiation (UVA) [11-13].

Betacarbolines belong to the interesting class of molecules potentially able to phototautomerise. Thus, as Scheme 1 shows, betacarbolines possess a very weak acidic pyrrolic group ($pK_a \approx 16$) and a moderately basic pyridinic nitrogen atom ($pK_a \approx 7$) [14]. The electronic excitation to the lowest singlet excited state strengthens the acidity and basicity of these centres around 4 and 7 pK_a units, respectively [14]. Accordingly, it has been proposed that, upon light absorption, betacarbolines can experience double excited state proton transfer reactions to give phototautomers of presumed zwitterionic structures [15, 16]. Although the phototautomerism of betacarbolines has been extensively studied for many years, its mechanism is still a subject of considerable speculation [17-25]. One of the most fundamental questions to resolve is whether the excited state proton transfer reactions proceed in a concerted fashion or by a stepwise mechanism.

A. S. Coronilla · C. Carmona · M. A. Muñoz · M. Balón (✉)
Departamento de Química Física, Facultad de Farmacia,
Universidad de Sevilla,
Sevilla 41012, Spain
e-mail: balon@us.es

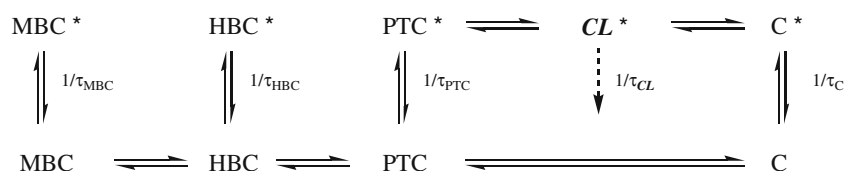


Scheme 1 Structural formulae of BC and MBC

Another is the nature of the presumed zwitterionic tautomers [26–28].

To get a better comprehension of the prototropic reactions of the betacarbolines, we have carried out in recent years a research program aimed to study the ground and excited state hydrogen bonding and proton transfer reactions of the N-methyl derivatives of betacarboline with different proton donors and acceptors in aprotic solvents [29–33]. The methylation in these substrates of the pyrrolic or pyridinic nitrogen atoms allows the separate study of the mechanisms and the factors influencing the protonation and deprotonation reactions of the betacarboline ring. These studies have demonstrated that the ground and excited state proton transfer reactions of the N-methyl betacarboline derivatives take place in aprotic solvents through complex stepwise mechanisms involving different hydrogen bonded adducts and exciplexes. Thus, the mechanism depicted in Scheme 2 for the interactions of N₉-methylbetacarboline, MBC, with the strong hydrogen bond donor 1,1,1,3,3,3-hexafluoroisopropanol, HFIP, typically summarised the results of our studies on the betacarboline pyridinic protonation in aprotic solvents [33].

As Scheme 2 shows, the protonation mechanism of MBC by HFIP in cyclohexane initially involves the formation, at very low concentrations of the donor, of a ground state hydrogen bonded complex, HBC, which, at higher concentrations of the donor, evolves to its ion-pair proton transfer complex, PTC. Upon excitation, the PTC reacts with another donor molecule to give the exciplex, CL*, the precursor of the excited state cation, C*. In a more polar media, as a 20% v/v toluene-cyclohexane mixture, ground state cations, C, are also formed. The direct excitation of these species also contributes to increase the excited state C* population.



Scheme 2 Protonation mechanism of MBC by HFIP in cyclohexane

Because of the fundamental role of water as solvent in chemical and biological processes, we thought interesting to extend these previous studies to check if the stepwise mechanism proposed in low polar aprotic solvents is also operative in aqueous media. However, since the water molecules in aqueous media play a double role as solvent and proton donor, the photophysical studies of hydrogen bonding interactions and proton transfer processes in bulk water are much more complicated than in the aprotic media. Moreover, the tendency of water molecules to self-aggregate in clusters of different sizes and structures blurs the description, at the molecular level, of the solute-water interactions and the dynamics of the proton transfer processes. Thus, owing to the complex nature of water, we thought advisable to begin our study on the aqueous MBC protonation equilibrium using mixed water-organic solvents instead of bulk water. These media can provide a straightforward way to model the water-betacarboline interactions by changing the water concentration in a controlled fashion.

Bearing this idea in mind, we have examined the influence of water concentration on the absorption and fluorescence spectra of MBC in different water co-solvent mixtures such as, water-diethylamine, water-dimethylsulfoxide, water-dioxane and water-N,N-dimethylformamide. These studies revealed that, in all these solvent mixtures, upon increasing the water concentration, the absorption and fluorescence spectra of MBC experience similar gradual changes. Therefore, after this previous scrutiny, we have selected the water-N,N-dimethylformamide system, water-DMF, as a representative media to carry out a thoroughly study of the ground and excited state proton transfer reactions of MBC in aqueous media. This paper reports the results of this study.

Experimental

MBC was prepared as described elsewhere [34]. Spectral grade DMF was used as co-solvent. Doubly distilled water was used thoroughly. Solutions of MBC in water-DMF mixtures for spectroscopic measurements were freshly prepared and were kept in the dark to avoid photodecomposition. Because the quenching by molecular oxygen was checked to be negligible, the measurements were carried

out with non-degassed solutions under temperature-controlled conditions, $25.0 \pm 0.1^\circ\text{C}$.

The UV-vis absorption spectra were recorded on a Cary 100 spectrophotometer and stationary fluorescence measurements in a Hitachi F-2500 spectrofluorometer using Spectrosil quartz cells of 1 cm path length. Dilute solutions of MBC ($\approx 10^{-5}\text{M}$) were used to avoid inner filter effects and re-absorption phenomena. The Peak Fit[®] Jandel Scientific Program was used to deconvolute the fluorescence spectra of MBC into their individual components. The emission bands were fitted to the logistic asymmetric function:

$$y = a_0(1 + \exp X)^{-(a_3+1)} a_3^{-a_3} (a_3 + 1)^{(a_3+1)} \exp X \quad (1)$$

with

$$X = -\frac{(x + a_2 \ln a_3 - a_1)}{a_2} \quad (2)$$

The amplitudes, a_0 , centres, a_1 , widths, a_2 , and shapes, a_3 of the convoluted bands were optimised with the Marquardt algorithm. The goodness of the fits was judged by the correlation coefficient and the visual inspection of the residuals.

The excitation spectra were recorded in a Perkin-Elmer spectrofluorometer 650-40 equipped with a data processor 650-0178. The spectra were corrected by measuring the instrumental response on the excitation side (rhodamine B) and on the emission side (cell diffuser). The time-resolved fluorescence measurements were performed with the time-correlated single photon counting FL900CD and Mini- τ spectrofluorimeters of Edinburgh Analytical Instruments. These instruments used as the excitation sources a hydrogen flash lamp and a picosecond laser diode, respectively. The fluorescence decay curves were acquired to $(1-2) \cdot 10^4$ counts in the peak and were fitted, by reconvolution analysis with the instrumental response function, to a sum of exponential functions with amplitudes, α_i , and lifetimes, τ_i .

$$I(t) = \sum \alpha_i \exp(-t/\tau_i) \quad (3)$$

The quality of the fits was analysed by the randomness of the residuals and the reduced chi-squares (χ^2). Global analyses of the fluorescence decays were performed using the standard program Level 2 based on the tried and tested Marquardt-Levenberg algorithm, supplied by Edinburgh Analytical Instruments.

Results

Figures 1 and 2 show the changes experienced by the absorption and fluorescence emission spectra of MBC upon

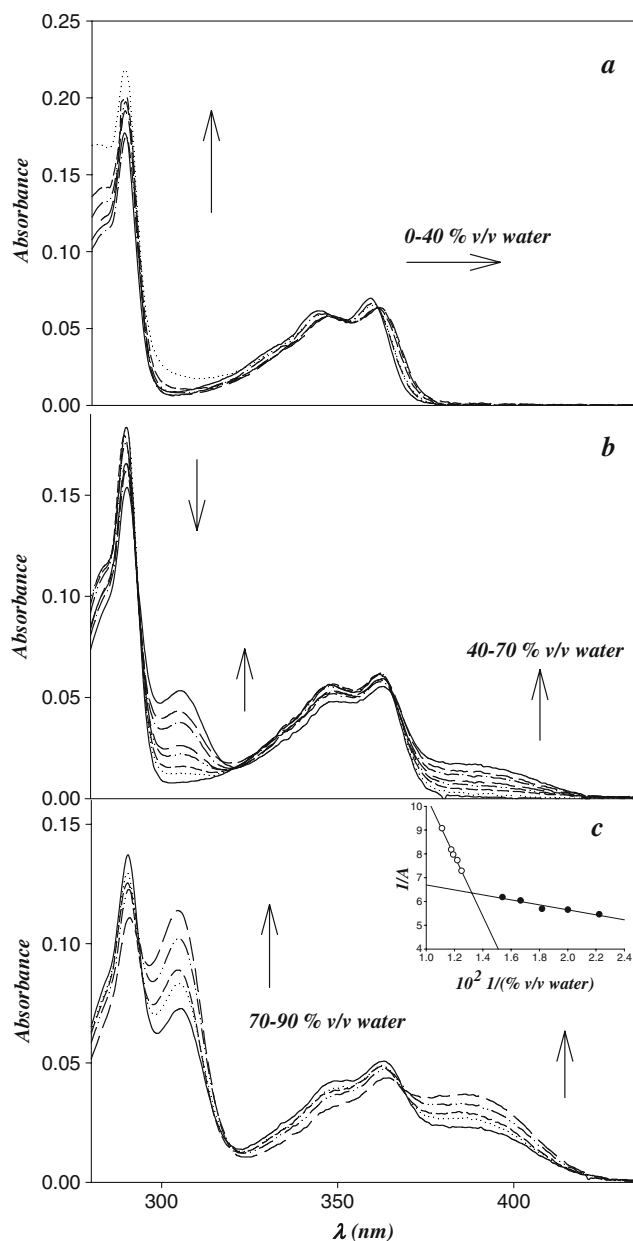


Fig. 1 Absorption spectra of MBC ($4 \cdot 10^{-5}\text{M}$) in water-DMF mixtures in the 0–40% v/v **a**, 40–70% v/v **b** and 70–90% v/v **c** ranges of water concentration. In the inset of Fig. 1c, the Benesi-Hildebrand plot of the reciprocal of the absorbances measured at 290 nm against the reciprocal of the water concentrations. Hereafter, the arrows indicate the direction of the spectroscopic changes upon increasing the water proportion of the water-DMF mixtures

increasing the water proportion of the water-DMF mixtures, respectively. These changes do not correlate with the slight increase experienced by the apparent pHs of the water-DMF mixtures upon the increase of the water proportion. It seems also rather unlikely that they could be due to preferential solvation effects. Conversely, these spectral changes, similar to those previously observed upon the addition of HFIP to MBC in cyclohexane [33], point out to

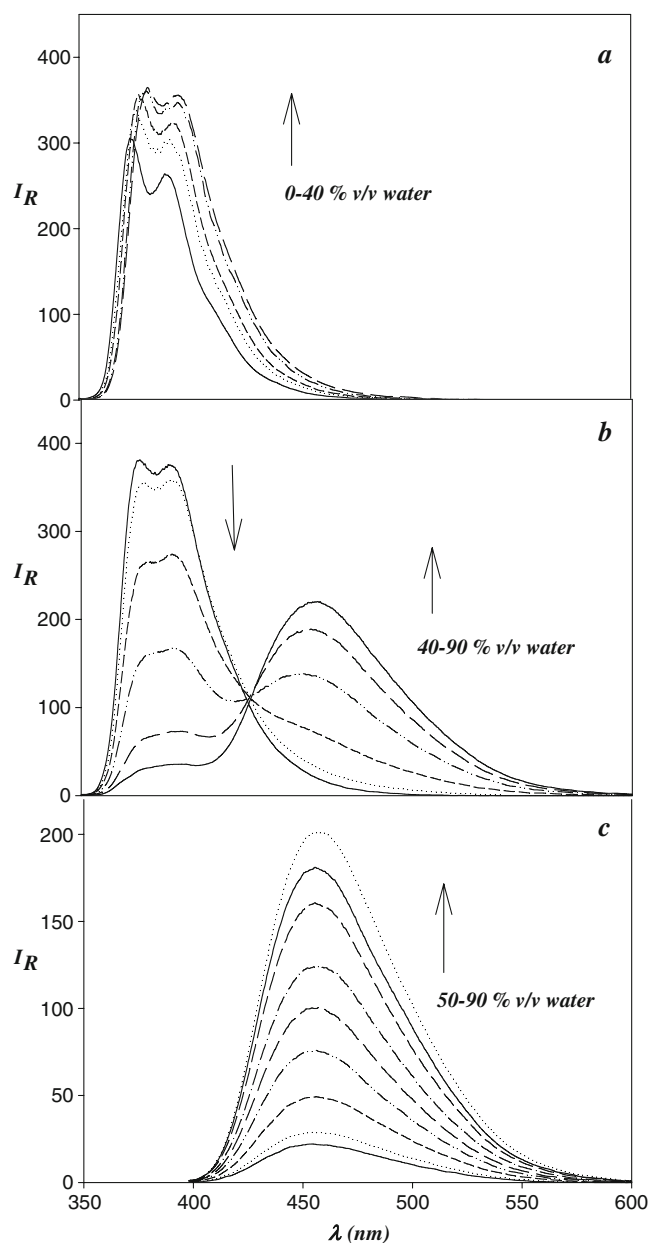


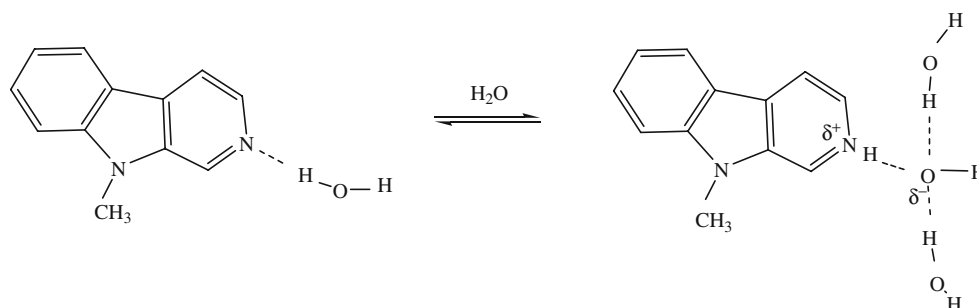
Fig. 2 Fluorescence emission spectra of MBC (4×10^{-5} M), $\lambda_{\text{exc}} = 325$ nm, in water-DMF mixtures of: **a** 0–40% v/v and **b** 40–90% v/v ranges of water concentration. **c** Fluorescence emission spectra of MBC in the 50–90% v/v water-DMF mixtures at $\lambda_{\text{exc}} = 390$ nm

the stepwise formation of different MBC-water adducts. Therefore, we will use the mechanism depicted in Scheme 2 as a guide to rationalise the spectral changes observed in the MBC-water-DMF system.

Thus, according to this mechanism, the changes observed in the absorption and emission spectra of MBC in the 0–40% v/v water-DMF mixtures upon increasing the water concentration, Figs. 1a and 2a, can be ascribed to the formation of a MBC-water hydrogen bonded complex $\text{N} \cdots \text{HOH}$, HBC, and its ion-pair proton transfer complex $\text{NH}^{\delta+} \cdots \text{O}^{\delta-} \text{H}$, PTC. The formation of the HBC, at very low water concentrations, does not practically affect the spectral characteristics of the neutral MBC. However, the further formation of the PTC, at higher water concentrations, produces the bathochromic shifts observed in the absorption and emission spectra of MBC. These spectral shifts can be attributed to the charge transfer between the pyrrolic and the pyridinic nitrogen atoms of the PTC.

As in the previous paper [33], the formation of the HBC and PTC complexes can be rationalised by postulating a double minimum potential for the position of the proton in the OHN bridge: one centred near to the oxygen atom of water and the other near to the pyridine nitrogen atom of the betacarboline ring. The driven force for the water catalysed $\text{HBC} \rightarrow \text{PTC}$ transformation would be the cooperative hydrogen bonding interactions between the water molecules [35, 36]. Thus, upon the HBC formation, the increase of the proton acceptor properties of the oxygen atom in the $\text{N} \cdots \text{H} \cdots \text{O}$ bridge makes this centre more prone to hydrogen bond with other water molecules. These hydrogen-bonding interactions weaken the water O–H bond of the $\text{O} \cdots \text{H} \cdots \text{N}$ bridge. The progressive weakening of this bond induces a gradual shift of the proton from the oxygen atom of water to the pyridinic nitrogen atom of the MBC. Therefore, according to this model, the PTC would have a structure similar to that of the 1:3 hydrogen bonded complex depicted in Scheme 3.

The changes experienced by the absorption and fluorescence spectra of MBC upon increasing the water concentration of the water-DMF mixtures above 40% v/v, are those expected for the formation of the MBC cationic



Scheme 3 Ground state HBC-PTC equilibrium

species [33]. Thus, in these media, the progressive growth of the absorption bands at 305 nm and 380–390 nm, Figs. 1b and c, and the emission band at 450 nm, Fig. 2b, typical of the MBC cations is observed. It is worthwhile to note that the fluorescence spectra obtained exciting the red edge of the MBC absorption spectra only show the cationic emission, Fig. 2c.

Because of the coexistence of different ground state MBC-water adducts, the MBC excitation spectra in these water-DMF mixtures are, as expected, strongly dependent on the water concentration and the monitored emission wavelength. However, it is particularly interesting to note the influence of the water concentration on the excitation spectra obtained by monitoring the emission of the cationic species at the red edge of the fluorescence spectra. Thus, as Fig. 3 typically shows, in the 50% v/v water-DMF mixture, the emission at 530 nm where the cations are the only emitting species, gives the typical excitation spectrum of the cationic species. However, in the 90% v/v water-DMF mixture, the excitation spectrum shows additional bands superimposed to the cationic spectrum. These results indicate that, whereas in the 50% v/v mixture the excited state cations, C*, are only formed from direct excitation of the ground state cations, in the 90% v/v mixture C* species are also formed from the excited state reaction of another ground state precursor.

The perusal of the MBC absorption spectra in the water-DMF mixtures above 40% v/v reveals that the absorption changes take place sequentially in two steps. Thus, the initial isosbestic point around 365 nm observed in the spectra of the 40–70% v/v water-DMF mixtures, Fig. 1b, further shifts to the red by 5 nm in the water-DMF mixtures of higher water concentrations, Fig. 1c. Moreover, as the inset in Fig. 1c typically shows, the double reciprocal plots

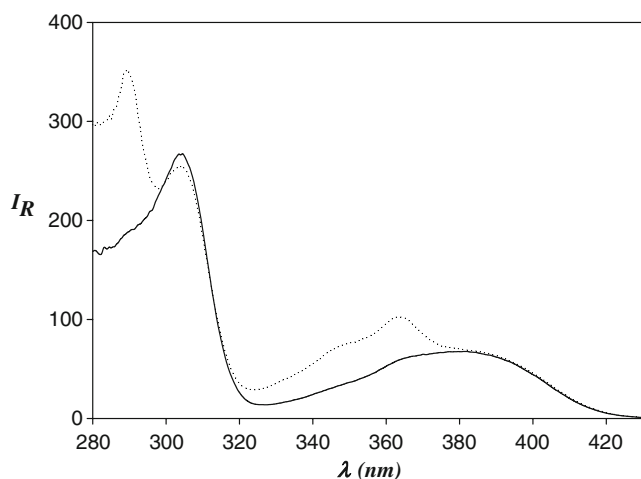


Fig. 3 Normalised MBC excitation spectra, $\lambda_{em}=530$ nm, in the 50% v/v (—) and 90% v/v (····) water-DMF mixtures

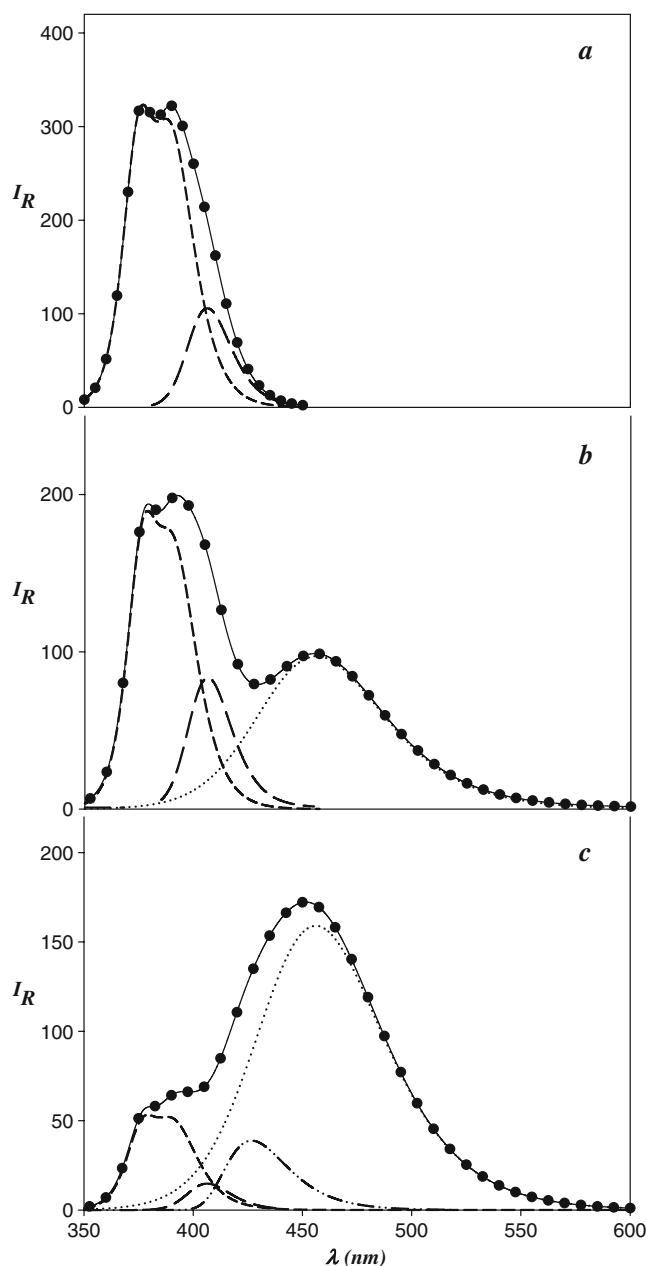


Fig. 4 Comparison of the experimental MBC emission spectra, $\lambda_{exc}=325$ nm, in the 30% v/v **a**, 65% v/v **b** and 85% v/v **c** water-DMF mixtures (dash lines) with those obtained (dotted lines) by reconvoluting the PTC(—), PC(—), CL (···) and C (····) emission spectra

of the absorbances against the water concentration render two straight lines whose slopes abruptly change. Therefore, these results show that the ground state cations, C, are not directly formed from the PTC, but from a new water-MBC adduct not previously observed in the MBC-HFIP system. Hereafter, this pre-cationic species will be named as PC.

Despite the absorption spectra provide founded proofs on the presence of the PC adduct, the fluorescence spectra do not apparently show any particular feature that can be

Table 1 Bi-exponential fluorescence decays, $\lambda_{\text{exc}}=330$ nm, of MBC in the 20–40% v/v water-DMF mixtures. The numbers between parentheses represent the relative percent contributions, f_i^a , of the decay components to the fluorescence signal

%v/v water	$\lambda_{\text{em}}/\text{nm}$	τ_1/ns	τ_2/ns	χ^2
20	380	5.7±0.3 (60)	7.6±0.2 (40)	1.189
20	420	5.5±0.5 (64)	7.8±0.2 (36)	1.120
30	380	5.4±0.6 (12)	7.7±0.3 (88)	1.165
30	420	5.7±0.3 (15)	7.6±0.2 (85)	1.172
40	380	5.6±0.3 (10)	7.8±0.2 (90)	1.145
40	420	5.7±0.2 (5)	7.6±0.3 (95)	1.098

^a $f_i=100 (\alpha_i\tau_i / \sum\alpha_i\tau_i)$ where α_i and τ_i are the pre-exponential factors and the decay times, respectively

attributed to the PC* emission. However, it seems rather unlikely that the PC* species be non-fluorescent. Conversely, it is more probable that the PC emission could be submersed into the emission bands of the PTC* or C* species. In this regard, it must be recalled that the profiles of the experimental fluorescence spectra of the MBC in cyclohexane solutions of sufficiently high HFIP concentrations, to exclude the presence of the HBC species, could be excellently reproduced by convoluting the emission bands of the PTC* (≈ 376 nm and 390 nm), CL* (≈ 420 nm) and C* (≈ 450 nm) species [31–33]. Therefore, the existence of the presumed submersed PC emission band could be revealed by a similar deconvolution analysis of the MBC fluorescence spectra in the water-DMF mixtures.

The results of this deconvolution analysis, Fig. 4, reveal that, as we presumed, to reproduce the experimental fluorescence spectra of MBC in the water-DMF mixtures, besides the mentioned PTC*, CL* and C* emission bands, an additional band around 400 nm is required. In consequence, this new band corresponds to the PC* emission. On the other hand, the convolution analyses also indicate that the cations begin to be formed in the DMF-water mixtures containing water proportions higher than 40% v/v. Thus, as Fig. 4a shows, in 40% v/v water-DMF, the experimental profiles of the emission spectra can still be

reproduced convoluting only the bands of the PTC and PC complexes. Moreover, in agreement with the results of our previous study on the MBC-HFPI system [33], to reproduce the experimental fluorescence spectra in the water-DMF mixtures of very high water concentrations, besides de PTC*, PC* and C* emission bands, the typical band at 420 nm of the CL* exciplex is necessary, Fig. 4c.

The time resolved fluorescence measurements definitively support the existence of the PC adducts. These measurements also allow to analyse the role played by this and the other MBC-water adducts and exciplexes in the mechanism of the betacarboline pyridinic protonation. These results could be roughly summarized as follows. In the water-DMF mixtures of very low water proportions, the MBC fluorescence decays are bi-exponential with very close decay times, around 3–4 ns. This behaviour is typical of the ground state HBC formation [30, 33]. However, in the 5–10% v/v water-DMF mixtures, the MBC fluorescence decays become mono-exponential with the lifetime around 5 ns typical of the PTC species [33]. This result indicates that, in these media, HBC has been completely transformed into PTC, but neither PC nor C species have been yet formed. As the water proportion of the water-DMF mixtures increases and the PC begins to be formed, the MBC fluorescence decays become again bi-exponential. As the data in Table 1 show, these fluorescence decays show an additional decay time component around 7–8 ns whose contribution to the fluorescence emission increases as the water concentration increases. Therefore, this decay time can be unambiguously assigned to the PC species.

In the water-DMF mixtures above the 40% v/v, once the MBC cations begin to be formed in the ground state, the fluorescence decays become more complex and, as expected, a long decay time component around 23 ns, typical of the betacarboline excited state cations, appears. The contribution of this decay time increases as the monitored emission wavelength and the water proportion of the water-DMF mixture increases. Worth noting, under these experimental conditions, the emissions of the MBC samples excited at the longer absorption wavelengths where only the PC and C species absorb decay bi-exponentially

Table 2 Pre-exponential factors, α_i , extracted from the global analysis ($\chi^2=1.142$) of the bi-exponential fluorescence decays, $\lambda_{\text{exc}}=380$ nm, of MBC in the 50–80% v/v water-DMF mixtures with linked decay times. The numbers between parentheses represent the relative percent contributions, f_i , of the decay components to the fluorescence signal

%v/v water	$\lambda_{\text{em}}/\text{nm}$	$\tau_1=27.0\pm 0.3\text{ns}$	$\tau_2=7.5\pm 0.4\text{ns}$	χ^2
50	420	0.007(20.2)	0.098 (79.8)	1.110
60	420	0.020 (39.8)	0.107 (60.2)	1.082
60	430	0.052 (73.0)	0.069 (27.0)	1.185
60	440	0.085 (90.7)	0.032 (9.3)	1.165
60	460	0.110 (99.7)	0.001 (0.3)	1.172
70	420	0.048(70.0)	0.074(30.0)	1.145
80	420	0.086(88.8)	0.039(11.2)	1.098

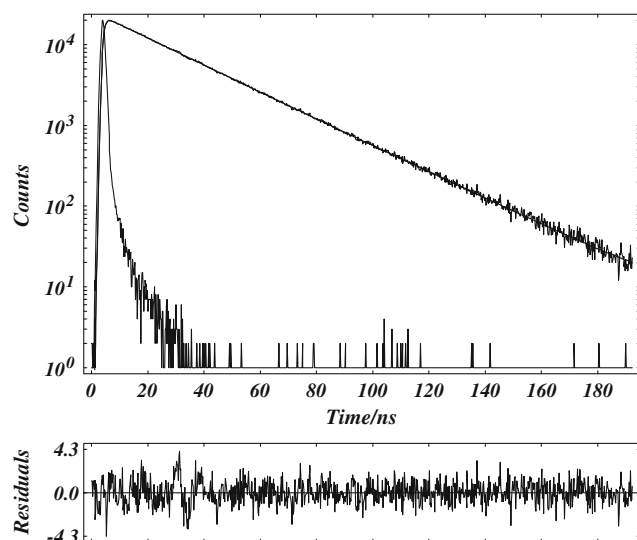


Fig. 5 Weighted residuals and autocorrelation function ($\chi^2=1.207$) for three-exponential analysis ($\tau_1=26.2$ ns and $\alpha_1=0.113$; $\tau_2=13.9$ ns and $\alpha_2=0.006$; $\tau_3=0.8$ ns $\alpha_3=-0.058$) of the fluorescence intensity decay of MBC in 90% v/v water-DMF mixture ($\lambda_{exc}=330$ nm, $\lambda_{em}=445$ nm)

with around 7 ns and 27 ns decay time components. Although the decay times do not practically change, their pre-exponential factors significantly change with the water proportion and the monitored emission wavelength. Thus, as the data reported in Table 2 show, upon increasing the water concentration of the water-DMF mixtures or the emission wavelength, the contribution of the PC* diminishes and that of the C* increases. Thus, the above fluorescence decay data show that PC* behaves as an independent fluorophore; namely, the PC* neither interacts with the PTC* nor with the C* species.

Finally, in the water-DMF mixtures with water concentrations over the 80% v/v, the MBC fluorescence decays at the emission wavelengths longer than 440 nm, where C* are the main emitting species, become three-exponential for most of the monitored excitation wavelengths, Fig. 5. Thus, for instance, as the data reported in Table 3 show, in the 90% v/v water-DMF mixture, the global analysis of the MBC fluorescence decays gives a long cationic decay time of 26.4 ± 0.4 ns, an intermediate decay time of 13.0 ± 0.6 ns, close to that of the CL* exciplex [33], and a rise time of

0.4 ± 0.2 ns. These results can be rationalised assuming that, as in the MBC-HFIP system, the excited state cations, C*, are formed in these water-DMF mixtures, through the PTC* \rightarrow CL* \rightarrow C* mechanism depicted in the Scheme 2. Accordingly, the short rise time of 0.4 ± 0.2 ns observed for the PTC* indicates that the PTC* \rightarrow CL* reaction efficiently competes with the PTC* radiative deactivation.

Discussion

Undoubtedly, the detection of the PC intermediate is the more relevant result of the present study. This result gives a new insight on the nature of the intermediates and the proton transfer mechanism of the pyridinic protonation of the betacarboline ring. Thus, the mechanism in Scheme 4, which includes the PC species, provides a better and more complete description of the different reaction pathways and intermediates involved in this protonation process.

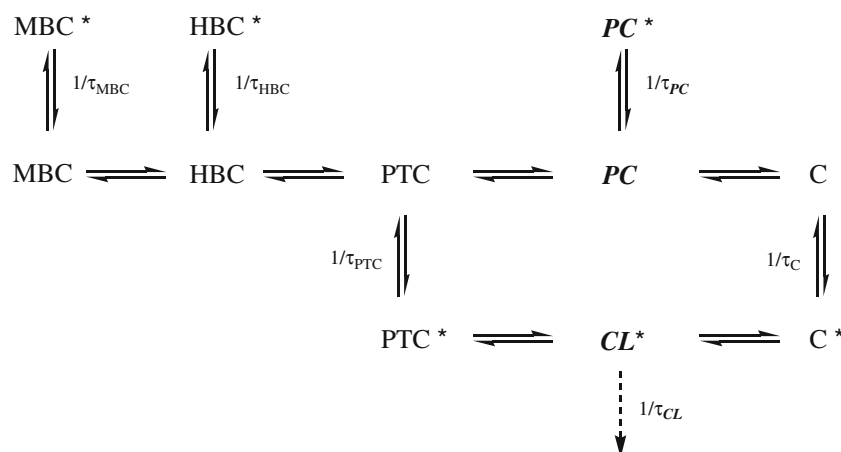
This mechanism assumes that the ground and excited state PTC \rightarrow C conversion takes place through two different intermediates; the PC in the ground state and the CL* in the excited state. Accordingly, the relative relevance of the ground and excited state PTC reactions and, therefore, the particular characteristics of the MBC protonation process in the different media, will vary depending on the proton donor and the solvent properties. Thus, in the case of the MBC-water-DMF system, contrarily to the MBC-HFIP system, the pyridinic protonation of the betacarboline ring seems to be much more favoured in the ground than in the excited state. As we will discuss below, the differences between the HFIP-MBC and water-MBC systems can be rationalised by considering the different hydrogen bond donor strengths of HFIP and water and the distinct solvating power of cyclohexane and water-DMF media.

As depicted in Scheme 4, the ground state pyridinic protonation of the betacarboline ring by water occurs by a stepwise mechanism involving the sequential formation of different hydrogen bonded MBC-water species. The increasing number of water molecules in the MBC-water adducts modulates the proton transfer process. The global number of water molecules required for the ground state

Table 3 Pre-exponential factors, α_i , extracted from the global analysis ($\chi^2=1.152$) of the three-exponential fluorescence decays of MBC in 90% v/v water-DMF with linked decay times

λ_{em}/nm	$\tau_1=26.4\pm 0.4\text{ns}$	$\tau_2=13.0\pm 0.6\text{ns}$	$\tau_3=0.4\pm 0.2\text{ns}$	χ^2
440 ^a	0.108	0.008	-0.030	1.218
440 ^b	0.111	0.004	-0.064	1.148
445 ^a	0.114	0.002	-0.094	1.020
445 ^b	0.111	0.005	-0.094	1.103
450 ^a	0.108	0.007	-0.013	1.183
450 ^b	0.111	0.006	-0.027	1.164

^a $\lambda_{exc}=325$, ^b $\lambda_{exc}=330$ nm



Scheme 4 Ground and excited state mechanisms of the water assisted MBC pyridinic protonation

MBC protonation might be roughly estimated as follows. The ground state equilibrium of MBC protonation can be expressed as:



being the equilibrium constant, K_C :

$$K_C = \frac{[\text{C}]}{[\text{MBC}][\text{H}_2\text{O}]^n} \quad (5)$$

Taking logarithms and rearranging we obtain:

$$\ln \frac{[\text{C}]}{[\text{MBC}]} = \ln K_C + n \ln [\text{H}_2\text{O}] \quad (6)$$

If the samples are excited at 390 nm and the emission recorded at 460 nm, where the cations are the main absorbing and emitting species, respectively, it can be assumed that the excited state cationic population is almost exclusively due to the excitation of the ground state cations. Under these experimental conditions, the intensity of the cationic fluorescence, A , would be linearly related with the ground state concentration of the cationic species. Straight-forward considerations let us transform the Eq. (6) to obtain:

$$\ln \frac{A}{A_0 - A} = \ln K_C + n \ln [\text{H}_2\text{O}] \quad (7)$$

where A_0 represents the fluorescence intensity of the MBC in an aqueous solution of pH=1 where the ground state protonation of MBC is complete. As Fig. 6 shows, the experimental results excellently fit Eq. (7), yielding a value for n close to 8 and an apparent global formation constant, K_C , value of $8 \pm 1 \cdot 10^{-10} \text{M}^{-8}$.

The high number of water molecules required for the MBC protonation is consistent with the currently accepted idea that the formation of water clusters is essential for the

proton transfer process [37–43]. Thus, on the one hand, the formation of the water clusters stabilizes the conjugated acid or basic counterpart. On the other hand, the hydrogen bonded water molecules in the clusters function as proton wires for the sequential hopping of the protons via a Grotthuss like process [44]. Thus, it is not the proton itself but its charge that is transferred through the pre-existing reaction coordinate provided by the water molecule hydrogen bonded to the substrate.

Noteworthy, the recent theoretical calculations of M.C. Sicilia and col. have demonstrated that clusters with more than four water molecules are required for the gas phase protonation of pyridine [45, 46]. In these pyridine- $n\text{H}_2\text{O}$ complexes, the water molecules of the cluster form two rings. Water molecules exclusively form the outer ring, whereas the inner ring also involves the

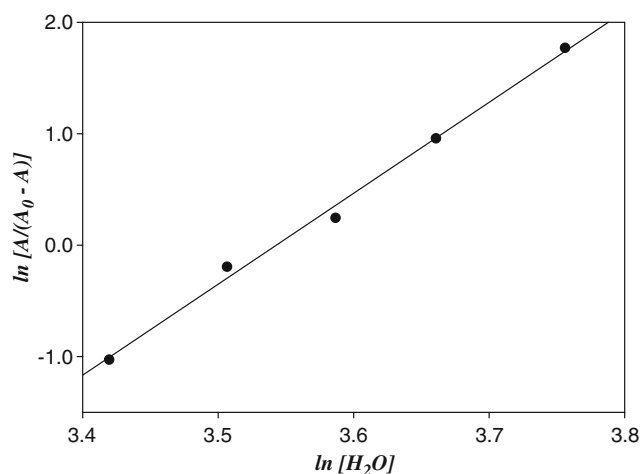
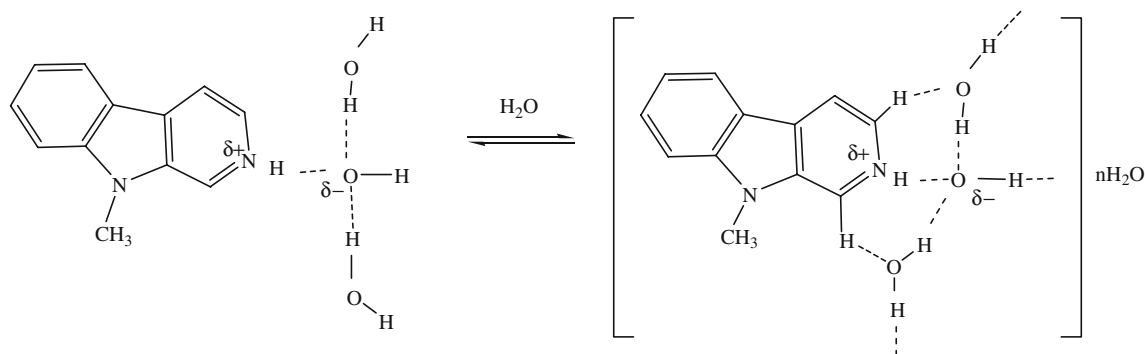


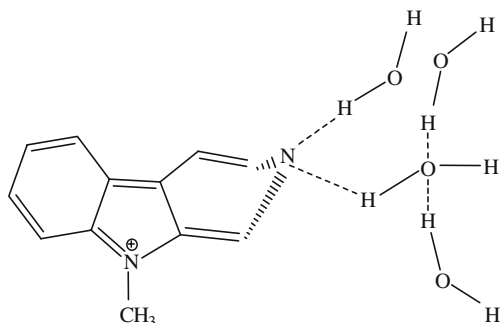
Fig. 6 Plot according to Eq. (7) of fluorescence intensities obtained by exciting the water-DMF mixtures at 390 nm and monitoring the emission at 460 nm



Scheme 5 Ground state PTC-CL equilibrium

pyridine molecule. The water molecules of the inner ring are hydrogen bonded to the pyridine nitrogen atom and the CH hydrogen atoms in ortho position to this centre. Thus, according to these theoretical results the structure for the PC depicted in Scheme 5 can be tentatively proposed. This structure allows rationalising the PTC \rightarrow PC reaction and the different ground state reactivity of the HFIP-MBC and water-MBC systems.

Thus, the model in Scheme 5 assumes that the PTC \rightarrow PC transformation implies the formation of the inner water-pyridine ring predicted by the theoretical calculations. This process involves the hydrogen bonding interactions between the oxygen atoms of the loose water molecules in the PTC and the CH hydrogen atoms in ortho position to the pyridinic nitrogen atom. Evidently, the positive charge density on the pyridinic nitrogen atom of the PTC would play a key role in this process, since it greatly enhances the weak hydrogen bond donor properties of the CH groups. On the other hand, based on this model and taking into account the good hydrogen bond acceptor properties of the water oxygen atoms, it is easy to explain why this ground state process is highly favoured in the water-DMF mixtures. Conversely, the extremely low hydrogen bond acceptor properties of the HFIP oxygen atom importantly hinder the PC formation.



Scheme 6 Tentative structure of the CL* exciplex

Surprisingly, despite the crucial role played by the PC species in the ground state MBC pyridinic protonation, they do not share in the MBC excited state protonation reaction. Thus, according to the mechanism in Scheme 4, C* species are formed from the excited state reaction of the PTC through the CL* exciplexes. Therefore, it is intriguing that the PC does not interact in the excited state neither with C* nor CL*. This fact could be explained assuming that the PTC experiences profound structural changes upon excitation. In this regard, it must be recalled that pyridine has a non-planar boat-shaped geometry in its singlet-excited state [45, 46]. Evidently, the excited state PTC* \rightarrow PC* transformation would be completely hindered if the pyridine ring of the PTC* would have a similar non-planar geometry.

The hypothesis of a non-planar boat-shaped geometry for the PTC pyridinic ring results very attractive. Thus, it allows to tentatively assign to the CL* exciplex the non-planar quinoid structure in Scheme 6. Thus, the excited state $sp^2 \rightarrow sp^3$ rehybridisation of the PTC pyridinic nitrogen atom makes this centre prone to hydrogen bond with an additional donor molecule. On the other hand, this hypothesis also allows to nicely explaining the different excited state reactivity of the HFIP-MBC and the water-MBC systems. Thus, the PTC* of the HFIP-MBC system is much more reactive than that of the water-MBC system, because HFIP is a better hydrogen bond donor than water [47].

To conclude, the results of the present study show that the ground and excited state pyridinic protonation of MBC in water-DMF mixtures takes place, as in other low polar aprotic solvents, through a stepwise mechanism involving different spectroscopically detectable intermediates. The mechanism proposed in Scheme 4 reasonably accounts for the main features of the ground and excited state proton transfer processes of MBC in the different media. However, the nature of the proposed adducts and exciplexes remains, at present, rather speculative. Experimental and theoretical studies that could help to clarify this question are currently in progress.

Acknowledgements We gratefully acknowledge financial support from the Dirección General Científica y Técnica MEC, CTQ2006-13539 and Junta de Andalucía, 2005/FQM-368, 2007/FQM-106.

References

- Abramovitch RA, Spencer ID (1964) The carbolines. *Adv. Heterocycl. Chem.* 3(1):79–207. doi:10.1016/S0065-2725(08)60542-5
- Allen JRF, Holmstedt BR (1980) The simple 3-carboline alkaloids. *Phytochem* 19:1573–1982. doi:10.1016/S0031-9422(00)83773-5
- Balón M, Muñoz MA, Guardado P, Hidalgo J, Carmona C (1994) Photophysics and photochemistry of betacarbolines. *Trends Photochem. Photobiol.* 3(1):117–138
- Bloom H, Barchas J, Sandler M, Usdin E (1982) Beta-carbolines and Tetrahydroisoquinolines, *Progress in Clinical and Biological Research.* Vol 90. Alan R. Liss Inc, New York
- Braestrup C, Nielsen M, Olsen CE (1980) Urinary and brain β -carboline-3-carboxylates as potent inhibitors of brain benzodiazepine receptors. *Proc. Natl. Acad. Sci. USA* 77(4):2288–2292. doi:10.1073/pnas.77.4.2288
- Carlini EA (2003) Plants and the central nervous system. *Pharmacol. Biochem. Behav.* 75(3):501–512. doi:10.1016/S0091-3057(03)00112-6
- Meester C (1995) Genotoxic potential of β -carbolines: a review. *Mutat. Res.* 339:139–153
- Tamura S, Konakahara T, Komatsu H, Ozaki T, Ohta Y, Takeuchi H (1998) Synthesis of β -carboline derivatives and their interaction with duplex-DNA. *Heterocycles* 48(12):2477–2480
- Balón M, Muñoz MA, Carmona C, Guardado P, Galán M (1999) A fluorescence study of the molecular interactions of harmine with the nucleobases, their nucleosides and mononucleotides. *Biophys. Chem.* 80(1):41–52. doi:10.1016/S0301-4622(99)00059-9
- Cao R, Peng W, Chen H, Ma Y, Liu X, Hou X, Guan H, Xu A (2005) DNA binding properties of 9-substituted harmine derivatives. *Biochem. Biophys. Res. Commun.* 338(3):1557–1563. doi:10.1016/j.bbrc.2005.10.121
- Hudson JB, Towers GH (1991) Therapeutic potential of plant-photosensitizers. *Pharmacol. Ther.* 49(3):81–122. doi:10.1016/0163-7258(91)90055-Q
- Shimoi K, Kawabata H, Tomita I (1992) Enhancing effect of heterocyclic amines and β -carbolines on UV or chemically induced mutagenesis in *E. coli*. *Mutat. Res.* 268(2):287–295. doi:10.1016/0027-5107(92)90234-S
- Guan H, Liu X, Peng W, Cao R, Ma Y, Chen H, Xu A (2006) β -Carboline derivatives: Novel photosensitizers that intercalate into DNA to cause direct DNA damage in photodynamic therapy. *Biochem. Biophys. Res. Commun.* 342(3):894–901. doi:10.1016/j.bbrc.2006.02.035
- Balón M, Hidalgo J, Guardado P, Muñoz MA, Carmona C (1993) Acid–base and spectral properties of betacarbolines. Part 2. Dehydro and fully aromatic betacarbolines. *J. Chem. Soc., Perkin Trans.* 2:99–104. doi:10.1039/p29930000099
- Sakuros R, Ghiggino KP (1982) Excited state proton transfer in betacarboline. *J. Photochem.* 18(1):1–8. doi:10.1016/0047-2670(82)80002-6
- Wolfbeis OV, Furlinger E, Wintersteiger R (1982) Solvent and pH-dependence of the absorption and fluorescence spectra of Harman: Detection of three ground state and four excited state species. *Monatsh. Chem.* 113:509–517. doi:10.1007/BF00799926
- Dias A, Varela AP, Miguel MG, Maçanita AL, Becker RS (1992) Beta-carboline photosensitizers 1. Photophysics, kinetics and excited-state equilibria in organic solvents, and theoretical calculations. *J. Phys. Chem.* 96(25):10290–10296. doi:10.1021/j100204a036
- Draxler S, Lippitsch ME (1993) Excited-state acid-base kinetics and equilibria in norharman. *J. Phys. Chem.* 99(44):11493–11496. doi:10.1021/j100146a024
- Varela AP, Dias A, Miguel MG, Becker RS, Maçanita AL (1995) Comment on excited-state acid-base kinetics and equilibria in Norharmane. *J. Phys. Chem.* 99(7):2239–2240. doi:10.1021/j100007a065
- Draxler S, Lippitsch ME (1995) Reply to “Comment on excited-state acid-base kinetics and equilibria in Norharmane”. *J. Phys. Chem.* 99(7):2241. doi:10.1021/j100007a066
- Dias A, Varela AP, Miguel MG, Becker RS, Burrows HD, Maçanita AL (1996) β -carbolines. 2. Rate constants of proton transfer from multiexponential decays in the lowest singlet excited state of harmine in water as a function of pH. *J. Phys. Chem.* 100:17970–17977. doi:10.1021/jp961406u
- Reyman D, Pardo A, Poyato JML (1994) Phototautomerism of betacarbolines. *J. Phys. Chem.* 98(41):10408–104110. doi:10.1021/j100092a004
- Reyman D, Viñas MH, Poyato JML, Pardo A (1997) Proton transfer dynamics of norharmane in organic solvents. *J. Phys. Chem. A* 101(5):768–775. doi:10.1021/jp961742a
- Reyman D, Viñas MH (1999) Temperature effect on excited-state proton transfer reactions of β -carboline in different acetic-acid mixtures. *Chem. Phys. Lett.* 301(5–6):551–558. doi:10.1016/S0009-2614(99)00060-3
- Chou P-T, Liu YI, Wu GR, Shiabo MY, Yu WS (2001) Proton-transfer tautomerism of β -carbolines mediated by hydrogen-bonded complexes. *J. Phys. Chem. B* 105(43):10674–10683. doi:10.1021/jp011031z
- Sánchez-Coronilla A, Carmona C, Muñoz MA, Balón M (2006) Ground state isomerism and dual emission of the β -carboline anhydrobase (N₂-methyl)-H-pyrido[3, 4-b]indole in aprotic solvents. *Chem. Phys.* 327(1):70–76. doi:10.1016/j.chemphys.2006.03.032
- Sánchez-Coronilla A, Balón M, Muñoz MA, Carmona C (2008) Influence of hydrogen bonding in the ground and the excited states of the isomers of the β -carboline anhydrobase (N₂-methyl-9H-pyrido[3.4-b]indole) in aprotic solvents. *Chem. Phys.* 344(1):72–78. doi:10.1016/j.chemphys.2007.11.011
- Sánchez-Coronilla A, Balón M, Muñoz MA, Hidalgo J, Carmona C (2008) Ground state isomerism in betacarboline hydrogen bond complexes: the charge transfer nature of its large Stokes shifted emission. *Chem. Phys.* 351(1):27–32. doi:10.1016/j.chemphys.2008.03.025
- Balón M, Carmona C, Guardado P, Muñoz MA (1998) Hydrogen-bonding and proton transfer interactions between Harmane and trifluoroethanol in the ground and excited singlet states. *Photochem. Photobiol.* 67(4):414–419. doi:10.1111/j.1751-1097.1998.tb05220.x
- Carmona C, Galán M, Angulo G, Muñoz MA, Guardado P, Balón M (2000) Ground and singlet excited states hydrogen bonding interactions of betacarbolines. *Phys. Chem. Chem. Phys.* 2(22):5076–5083. doi:10.1039/b005455k
- Carmona C, Balón M, Galán M, Angulo G, Guardado P, Muñoz MA (2001) Kinetic study of hydrogen bonded exciplex formation of N₉-methyl harmane. *J. Phys. Chem. A* 105(45):10334–10338. doi:10.1021/jp0104942
- Carmona C, Balón M, Galán M, Guardado P, Muñoz MA (2002) Dynamic study of excited state hydrogen-bonded complexes of harmine in cyclohexane-toluene mixtures. *Photochem. Photobiol.* 76(3):239–246. doi:10.1562/0031-8655(2002)076<0239:DSOESH>2.0.CO;2
- Carmona C, Balón M, Sánchez Coronilla A, Muñoz MA (2004) New insights on the excited-state proton-transfer reactions of

- betacarbolines: Cationic exciplex formation. *J. Phys. Chem. A* 108:1910–1918. doi:10.1021/jp030829a
34. Doig, G.G., Loudon, J.D., Mac Closkey, P.J.: The chemistry of the *Mitragyna* Genus. Part IV: Derivatives of Harman. *J. Chem. Soc.* 3912–3916 (1952) doi:10.1039/jr9520003912
35. Frank HS, Wen WY (1957) Structural aspects of ion-solvent interaction in aqueous solutions: a suggested picture of water structure. *Discuss. Faraday Soc.* 24:133–140. doi:10.1039/df9572400133
36. Gutmann V (1973) Redox properties: changes effected by coordination. *Struct Bonding* 15:141–166. doi:10.1007/BFb0036785
37. Lee J, Robinson GW, Webb SP, Philips LA, Clark JH (1986) Hydration dynamics of protons from photon initiated acids. *J. Am. Chem. Soc.* 108(21):6538–6542. doi:10.1021/ja00281a016
38. Robinson GW, Thidhethwhite PJ, Lee J (1986) Molecular aspects of ionic hydration reactions. *J. Phys. Chem.* 90(18):4224–4233. doi:10.1021/j100409a003
39. Lee J, Griffin RD, Robinson GW (1985) 2-Naphthol: A simple example of proton transfer affected by water structure. *J. Chem. Phys.* 82(11):4920–4925. doi:10.1063/1.448665
40. Solntsev KM, Huppert D, Agmon N, Tolbert LM (2000) Photochemistry of “super” photoacids. 2. Excited-state proton transfer in methanol/water mixtures. *J. Phys. Chem. A* 104(19):4658–4669. doi:10.1021/jp994454y
41. Agmon N (2005) Elementary steps in excited-state proton transfer. *J. Phys. Chem. A* 109(1):13–35. doi:10.1021/jp047465m
42. Mohammed OF, Pines D, Dreyer J, Pines E, Nibbering ETJ (2005) Sequential proton transfer through water bridges in acid-base reactions. *Science* 310:83–86. doi:10.1126/science.1117756
43. Siwick BJ, Bakker HJ (2007) On the role of water in intermolecular proton-transfer reactions. *J. Am. Chem. Soc.* 129(44):13412–13420. doi:10.1021/ja069265p
44. de Grotthuss CJT (1806) Sur la décomposition de l’eau et des corps qu’elle tient en dissolution à l’aide de l’électricité galvanique. *Ann Chim* 58:54–73
45. Sicilia MC, Muñoz-Caro C, Niño A (2005) Theoretical analysis of pyridine protonation in water clusters of increasing size. *Chem-PhysChem* 6(1):139–147. doi:10.1002/cphc.200400344
46. Sicilia MC, Niño A, Muñoz-Caro M (2005) Mechanism of pyridine protonation in water clusters of increasing size. *J. Phys. Chem. A* 109(37):8341–8347. doi:10.1021/jp050530n
47. Marcus Y (1993) The properties of organic liquids that are relevant to their use as solvating solvents. *Chem. Soc. Rev.* 22:409–416. doi:10.1039/cs9932200409